Analytical Approach in Finding the Semi-Optimum Hollow-Core Bragg Fiber with Minimum Loss

Amir M. Jazayeri, *Member, IEEE*, and Khashayar Mehrany, *Member, IEEE*

***Abstract*— Since it is quite difficult to analytically optimize hollow-core Bragg fibers to have minimum confinement loss without using the Floquet theorem, which does not hold for cylindrical structures, the cylindrical Bragg mirror is approximated by its planar counterpart. For this reason, first, the optimum planar waveguide formed by sandwiching a hollow layer between 1-D Bragg mirrors is found in this paper. The optimization for the dominant transverse-electric mode is analytically performed by using the pointwise wavenumber closely related to the wave admittance. A closed-form expression is then found to relate the propagation constant of this waveguide to the thickness of the hollow layer. This expression is then modified for the cylindrical structure, and the propagation constant is approximately related to the hollow-core diameter of the Bragg fiber to be optimized. The optimum cladding region is then found as if it were planar and a semi-optimum hollow-core Bragg fiber is proposed. Its superiority over conventional hollow-core Bragg fibers is numerically demonstrated by following a rigorous approach.**

***Index Terms*— 1-D photonic crystal, Bragg fiber, confinement loss.**

I. Introduction

OPTICAL fibers, as the main bed for optical communications, are usually engineered by introducing longitudinal or transverse periodic variations to control light propagation [1]. Hollow-core Bragg fibers; in particular, counts among the famous engineered fibers that exploit 1-D radial periodicity to guide light within a hollow-core fiber and thus to reduce the overall loss and nonlinearity. A typical hollow-core Bragg fiber whose cladding is periodically made of two materials with contrasting refractive indices is shown in Fig. 1(a). Being first proposed by Yeh *et. al*. in 1978 [2], it has been the subject of further studies [3], [4] and has found miscellaneous applications e.g. in light transmission [5], and dispersion compensation [6].

In this paper, our major concern is to minimize the confinement loss of this type of optical fibers by pursuing an analytical approach. It should be noticed that every realistic hollow-core Bragg fiber inevitably contains only a finite number of layers and therefore suffers from an unsolicited radiation loss. The good side of this unwanted leakage of power is that a multimode fiber can be effectively rendered to a single-mode one supporting the TE_{01} mode, which sees the largest bandgap and so has the minimum loss [7]. It is the loss of the TE_{01} mode in a typical hollow-core Bragg fiber that is to be analytically minimized in this work.

On the face of it, this end can be achieved by rigorously describing the electromagnetic fields in terms of Hankel functions [8], and then extracting the imaginary part of the propagation constant [9] to have the confinement loss minimized. Unfortunately and despite the radial periodicity of the refractive index profile, the Floquet theorem does not hold in the nonplanar structure of the cladding. Obtaining a closed-form expression for the parameters of optimum hollow-core Bragg fiber, which is supposed to have the minimum loss, is therefore prohibited. A rigorous minimization of radiation loss in hollow-core Bragg fibers thus calls for a brute-force optimization technique, e.g. the genetic algorithm [10], unless an accurate enough approximation is made to ease the optimization process.

Replacing the Bragg fiber shown in Fig. 1(a) with its planar counterpart shown in Fig. 1(b) is such an approximation [11], [12]. Although the electromagnetic properties of the latter structure are somewhat different form the original cylindrical structure, it can provide a good enough description of guiding properties within the fiber and can simplify the minimization of the radiation loss by providing a Bloch wavenumber for the cladding region. It is worth noticing that the refractive index of core in these figures is denoted by n_c to preserve the generality of our discussion. It is obvious that we have $n_c = 1$ for hollow-core Bragg fibers.

Using the planar structure as a good enough approximation and for a given set of refractive indices n_1 and n_2, the optimum thicknesses d_1 and d_2 are analytically found to have the maximum value for the imaginary part of the Bloch wavenumber in the planar substitution of the cladding region. This is rigorously performed by using the admittance/impedance concept and interestingly, it is shown that the well-known quarter-wave stack (QWS) Bragg mirror does not have the minimum leakage loss. The optimum thicknesses in the planar structure are then employed for the cladding region in the original cylindrical structure and a semi-optimum hollow-core Bragg fiber is then designed.

The leakage loss of the dominant mode, TE_{01}, in the proposed semi-optimum design is orders of magnitude lower than the leakage loss in the hollow-core Bragg fiber under the QWS condition or the low-loss Bragg fiber presented in [5]. At the same time, the loss factor of EH_{11}, the nearest mode to TE_{01}, and the dispersion coefficient of the dominant mode in the semi-optimum design do not change significantly. It is also worth noticing that the loss in the proposed structure is not

Manuscript received October 28, 2010; revised December 27, 2010; accepted January 23, 2011. Date of current version April 1, 2011.

The authors are with the School of Electrical Engineering, Sharif University of Technology, Tehran 145888-9694, Iran (e-mail: amirjazayeri@ee.sharif.edu; mehrany@sharif.edu).

Digital Object Identifier 10.1109/JQE.2011.2109938

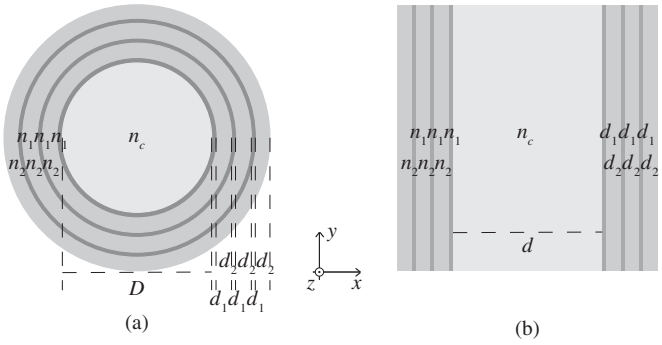

Fig. 1. (a) Bragg fiber with a radially periodic cladding with period $\Lambda = d_1 + d_2$, refractive indices and thicknesses are represented by the letters n and d, respectively. Note that $n_c = 1$ for a hollow-core fiber. (b) Corresponding planar structure. It is uniform along the y-axis.

lowered at the expense of having large thicknesses. Rather, the geometrical area of the proposed semi-optimum design happens to be smaller than that of the more conventional Bragg fibers.

The structure of this paper is therefore as follows. In section II, the planar counterpart of a typical Bragg fiber, i.e., a planar waveguide sandwiched by two semi-infinite 1-D Bragg mirrors, is studied to find the optimum parameters for maximizing the imaginary part of the Bloch wavenumber in the band-gap of the Bragg mirror. In section III, the semi-optimum Bragg fiber with an arbitrary core diameter is designed by using some of the parameters introduced in section II. First, the core diameter is related to the propagation constant of the structure and then the optimum planar Bragg mirror is found. The optimum planar structure, with its constituting parameters left intact, is rolled into a cylindrical shape and used as a cladding region to form a semi-optimum hollow-core Bragg fiber. In section IV, the semi-optimum structure is rigorously analyzed and the numerical results comparing its performance against conventional hollow-core Bragg fibers are presented. Finally, conclusions are made in section V.

II. Optimum Design for the Planar Counterpart

In this section, the planar surrogate structure of the fiber as depicted in Fig. 1(b) is optimized to attain the minimum possible loss. Alternating layers in the Bragg mirror region are made of lossless dielectrics with refractive indices n_L having thickness of d_L, and $n_H > n_L$ having thickness of d_H. It is obvious that in accordance with the figure, we have a 1-D Bragg mirror whose unit cell is made of a bilayer with refractive indices of $n_{1,2} = n_{H,L}$ or possibly $n_{1,2} = n_{L,H}$, and thicknesses of $d_{1,2} = d_{H,L}$ or possibly $d_{1,2} = d_{L,H}$. First, the Bloch wavenumber supported by the periodic repetition of adjacent low- and high-index regions is analytically extracted and then maximized to make sure that the radiation leakage loss originating from the exponential tail of the decaying field in the forbidden gap of the Bragg mirror is the least possible. Then, the appropriate core thickness; d, to support the highly confined Bloch wave is found and thus the optimum planar structure is designed. Throughout this article, the angular frequency of time harmonic fields, their corresponding wavenumber in vacuum, and the propagation constant along the z-axis are denoted by ω_0, k_0, and β_d, respectively. The analysis is provided for transverse-electric (TE) polarization, which is the polarization of the dominant mode we are interested in. It can be however easily modified to be applied for TM polarization.

A. Optimum Bragg Mirror

The Helmholtz equation for TE polarized waves in the Bragg mirror region reads as: $(\frac{d^2}{dx^2} + k_x^2)E_y = 0$, where $x \in (-\infty, +\infty)$, and $k_x(x) = k_{x_i} = \sqrt{n_i^2 k_0^2 - \beta_d^2}$ $(i = 1, 2)$ is a periodic piecewise constant function. According to the Bloch wave theorem, the electric field can be written as a superposition of two Bloch waves: $E_{y_{1,2}} = e^{-j\beta_d z} e^{j\kappa_{1,2} x} e_{y_{1,2}}(x)$, where $\kappa_{1,2}$ and $e_{y_{1,2}}(x)$ are the Bloch wavenumbers and their corresponding periodic functions, respectively. Depending on whether the angular frequency lies within or without the forbidden gaps, $\kappa_{1,2}$ can be written down as:

$$\kappa_{1,2} = \begin{cases} \frac{\pi}{\Lambda} \pm j\mu \quad (0 < \mu); & \begin{cases} \text{if } (\omega_0 \in 1^{st} \text{ band-gap}) \\ \text{or } (\omega_0 \in 3^{rd} \text{ band-gap}) \\ \text{or } \ldots \end{cases} \\ \pm j\mu \quad (0 < \mu); & \begin{cases} \text{if } (\omega_0 \in 2^{nd} \text{ band-gap}) \\ \text{or } (\omega_0 \in 4^{th} \text{ band-gap}) \\ \text{or } \ldots \end{cases} \\ \pm\tilde{\kappa} \quad (0 \le \tilde{\kappa} \le \frac{\pi}{\Lambda}); & \text{otherwise} \end{cases} \tag{1}$$

where $\Lambda = d_1 + d_2$ stands for the periodicity of the Bragg mirror, and, μ and $\tilde{\kappa}$ are both real numbers that can be obtained by solving the following band-diagram equation [13]:

$$\cos(\kappa_{1,2}\Lambda) = A \triangleq -\frac{1}{2}\sin(k_{x_1}d_1)\sin(k_{x_2}d_2)\left(\frac{k_{x_1}}{k_{x_2}} + \frac{k_{x_2}}{k_{x_1}}\right) + \cos(k_{x_1}d_1)\cos(k_{x_2}d_2). \tag{2}$$

It should be noticed that the three different scenarios for the Bloch wavenumber given in (1) correspond to $A < -1$, $1 < A$, and $-1 \le A \le 1$, respectively.

At this point, it is extremely difficult to find the optimum thicknesses d_1 and d_2 for maximizing the imaginary part of the Bloch wavenumber, i.e. μ. For this reason, a new function $p = -\frac{\frac{dE_y}{dx}}{E_y}$ that was introduced in [11] is here employed to substitute d_1 and d_2 with p_1 and p_2, viz. the values of this function at the interfaces between the higher- and lower-index layers. This is schematically shown in Fig. 2(a). In this manner, the maximum localization of Bloch waves in the Bragg mirror is attained by finding the optimum p_1 and p_2, which can later render the optimum thicknesses, d_1 and d_2. It is obvious that $p(x)$ is closely related to the Bloch wave admittance, $\frac{H_z}{E_y}$, along the x-axis and therefore is a continuous function of x except at those points, where the electric field is zero and $p(x)$ is singular. Such singularities correspond to short circuit conditions along transmission lines, where the impedance is zero and the admittance is infinite. Furthermore, this new function, in contrast to electromagnetic fields which

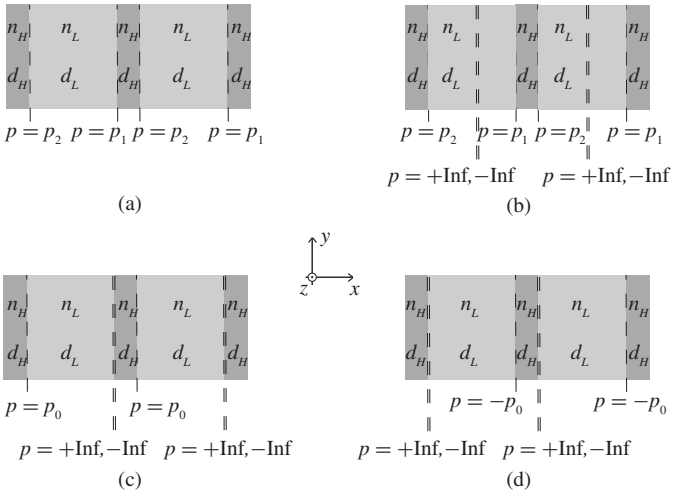

Fig. 2. Representation of pointwise wavenumber of a 1-D Bragg mirror at the interface between higher and lower index layers, p_1 and $p_2 > p_1$: (a) the most general case; (b) with one point of singularity within the lower index layer; (c) and (d) with one point of singularity at the interface between higher and lower index layers.

are Bloch-periodic waves, is strictly periodic with a period of $\Lambda = d_1 + d_2$, and satisfies $\frac{dp}{dx} = p^2 + k_x^2$. Since $p(x)$ has the dimension of length inverse, it is hereafter referred to as the pointwise wavenumber.

Although our work is limited to TE polarization, it is worth noticing that the pointwise wavenumber for TM polarized waves would have been $q = -\frac{\frac{dH_y}{dx}}{n^2 H_y}$, which is closely related to the Bloch wave impedance, $\frac{E_z}{H_y}$, and satisfies $\frac{dq}{dx} = n^2 q^2 + \frac{k_x^2}{n^2}$, where n stands for the periodic refractive index profile.

Getting back to the TE polarization case, the following two equations are very easy to obtain:

$$dx = \frac{dp}{p^2 + k_x^2} \tag{3}$$

$$\frac{dE_y}{E_y} = -\frac{pdp}{p^2 + k_x^2}. \tag{4}$$

Now, given that $p(x)$ is not a complex function whenever ω_0 lies within a band-gap, the abovementioned equations can be integrated and written as:

$$x_2 - x_1 = \int_{p(x_1)}^{p(x_2)} \frac{dp}{p^2 + k_x^2} \tag{5}$$

$$\left|E_y(x_2, y_0, z_0)\right| = \left|E_y(x_1, y_0, z_0)\right| e^{-\int_{p(x_1)}^{p(x_2)} \frac{pdp}{p^2 + k_x^2}} \tag{6}$$

where x_1, x_2, y_0, and z_0 are coordinates of two arbitrary points within every single layer.

There are now three different possible cases. The first is when $0 \le \beta_d < n_L k_0$. This is the most conventional case in a hollow-core waveguide because the propagation constant, β_d, should be less than k_0 to make sure that the electromagnetic fields are sinusoidal in the transverse plane. In this case, $k_x^2(x)$ is a periodic piecewise constant function, which takes only either of the two positive values $k_{H,L}^2 = n_{H,L}^2 k_0^2 - \beta_d^2$ ($0 < k_L < k_H$). The pointwise wavenumber, $p(x)$, will then be a monotonically increasing function because its derivative is always positive in accordance with equation (3). Therefore, it should have at least one singularity because it is also a periodic function. As already mentioned, these singularity points correspond to electric field zero points. The presence of more than one singularity point; however, decreases the imaginary part of the Bloch wavenumber and is thus not desirable. For the moment and in accordance with Fig. 2(b), it is assumed that the single singularity occurs in the lower-index layer, and then, it is shown that this single singularity should be at the interface between higher- and lower-index regions. To this end, the formulae given in (5) and (6) are further simplified when x_1 and x_2 represent the planar interface between the higher- and lower-index layers. Subsequently, the sought after parameter, μ, is obtained in terms of p_1 and p_2:

$$\pm\mu(p_1, p_2) = \frac{\frac{1}{2}\ln\left[\frac{(p_1^2+k_L^2)(p_2^2+k_H^2)}{(p_1^2+k_H^2)(p_2^2+k_L^2)}\right]}{\frac{1}{k_L}\tan^{-1}(\frac{p_1}{k_L}) - \frac{1}{k_H}\tan^{-1}(\frac{p_1}{k_H}) + \ldots}$$

$$\overline{\ldots \frac{1}{k_H}\tan^{-1}(\frac{p_2}{k_H}) - \frac{1}{k_L}\tan^{-1}(\frac{p_2}{k_L}) + \frac{\pi}{k_L}}.$$

Since there are no local extrema for this expression, the maximum value for μ is expected to occur when either p_1 or p_2 approaches infinity. There are only two imaginable cases which are depicted in Figs. 2(c) and 2(d). These two scenarios yield $+\mu$, when p_1 approaches infinity and p_2 is finite, and $-\mu$ when p_1 is finite and p_2 approaches infinity, respectively. If the finite value of $p(x)$ be named p_0 and $-p_0$, in the former and latter cases, respectively; then the maximum value of μ will be achieved whenever the following equation is held:

$$\frac{1}{2}\ln\left(\frac{p_0^2 + k_H^2}{p_0^2 + k_L^2}\right) = p_0\left[\frac{1}{k_H}\tan^{-1}\left(\frac{p_0}{k_H}\right) - \frac{1}{k_L}\tan^{-1}\left(\frac{p_0}{k_L}\right) + \frac{\pi}{2k_H} + \frac{\pi}{2k_L}\right]. \tag{7}$$

Under this condition, the maximum value of μ will interestingly be p_0, and the optimum thicknesses of higher- and lower-index layers will be given by the following expressions:

$$d_H = \frac{\pi}{2k_H} + \frac{1}{k_H}\tan^{-1}\left(\frac{p_0}{k_H}\right) \tag{8-a}$$

$$d_L = \frac{\pi}{2k_L} - \frac{1}{k_L}\tan^{-1}\left(\frac{p_0}{k_L}\right). \tag{8-b}$$

It is worth noticing that the difference between the here-proposed thicknesses and those of the QW design depends on β_d and is much more conspicuous for larger β_ds. The difference is however not negligible.

It should be however noticed that the imaginary part of the Bloch wavenumber is in this fashion maximized at a specified angular frequency ω_0. In other words, the optimum thicknesses given in (8-a) and (8-b) render the maximum achievable μ when n_H, n_L, ω_0 and β_d are all fixed and given. It is therefore not surprising if larger values of μ be encountered at some other frequencies other than ω_0. To drive this point home, a typical 1-D photonic crystal with $n_H = 4.6$, and $n_L = 1.6$ is considered at the free space wavelength $\lambda_0 = 1.55\ \mu m$ and

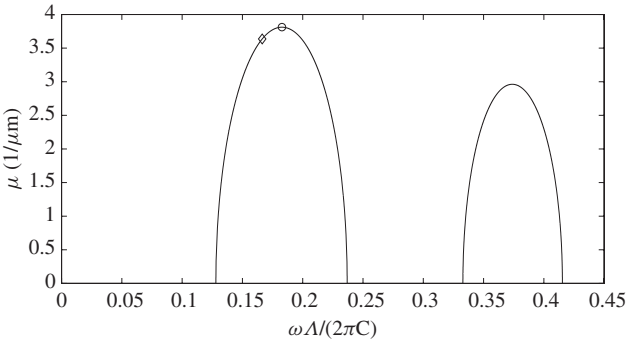

Fig. 3. TE imaginary parts of the Bloch wavenumber for a 1-D Bragg mirror with $n_H = 4.6$, $d_H \simeq 95$ nm, and $n_L = 1.6$, $d_L \simeq 163$ nm at $\beta_d = 0$ versus the normalized frequencies. The structure is designed to have the maximum Bloch confinement at the free-space wavelength $\lambda_0 = 1.55$ μm, and yet the imaginary part of the Bloch wavenumber reaches its maximum at $\lambda_0 = 1.411$ μm. These two points are depicted by a diamond and a circle, respectively. Although the imaginary part of the Bloch wavenumber at $\lambda_0 = 1.55$ μm is not the maximum value within the forbidden band, it is impossible to find a 1-D Bragg mirror of whatever thicknesses with $n_H = 4.6$ and $n_L = 1.6$ whose μ at $\lambda_0 = 1.55$ μm be larger than 3.636 μm^{-1}.

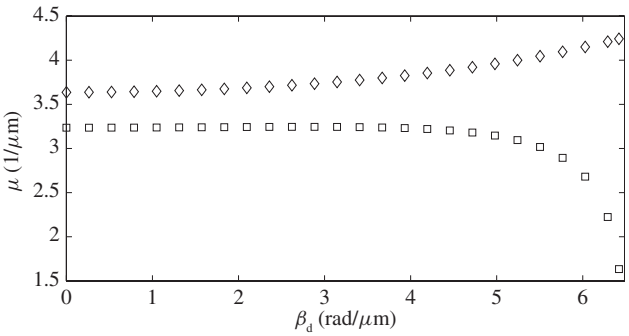

Fig. 4. TE imaginary part of Bloch wavenumber at $\lambda_0 = 1.55$ μm versus longitudinal propagation constant β_d for the optimum (diamond) and quarter-wave (square) structures having $n_H = 4.6$ and $n_L = 1.6$.

$\beta_d = 0$. The optimum thicknesses of higher- and lower-index layers are found to be $d_H \simeq 95\ nm$, and $d_L \simeq 163\ nm$, respectively. The imaginary part of the Bloch wavenumber supported by this specific photonic-crystal is plotted in Fig. 3. We can be sure that; no matter what are the thicknesses of higher and lower indices, d_H and d_L, there is no 1-D Bragg mirror at $\lambda_0 = 1.55\ \mu m$ and $\beta_d = 0$ with the same n_H and n_L, having a Bloch wavenumber whose imaginary part is larger than 3.636 μm^{-1}, i.e. the imaginary part of the Bloch wavenumber of the optimum structure with $d_H \simeq 95\ nm$ and $d_L \simeq 163\ nm$ marked by diamond in Fig. 3. This is not true at other frequencies as even the optimum structure itself has its maximum confinement at $\lambda_0 = 1.411\ \mu m$ at which the imaginary part of the Bloch wavenumber is 3.811 μm^{-1} marked by circle in the same figure.

To compare the performance of the optimum structure against other 1-D Bragg mirrors, QWS with the same n_H and n_L is also analyzed for $0 \le \beta_d < n_L k_0$ and the results are depicted in Fig. 4. In compliance with what was stated about the difference between the here-proposed thicknesses and those based on the QWS design, the difference between the imaginary part of the Bloch wavenumber in the here-proposed structure and the QWS becomes quite noticeable for higher β_ds. At the limit, when β_d approaches $n_L k_0$, μ tends to zero in the QWS and reaches its maximum at the here-proposed structure.

The second case is when $n_L k_0 < \beta_d < n_H k_0$. In the higher index layer, $k_x^2(x) = k_H^2 = n_H^2 k_0^2 - \beta_d^2$, is a positive number and thus $p(x)$ in that layer is always ascending. Although point singularities, i.e., electric field zeros, are allowed to exist in the high index region, they are avoided in the optimum design because they reduce the imaginary part of Bloch wavenumber. In the lower index layer, $k_x^2(x) = -\gamma_L^2 = n_L^2 k_0^2 - \beta_d^2$, is on the other hand a negative number and $p(x)$ in that layer is a one-to-one function. There are therefore two possibilities: we have either $-\gamma_L < p_1 < p_2 < \gamma_L$ (see Fig. 2(a)) when there is no singularity or $p_1 < -\gamma_L, \gamma_L < p_2$ (see Fig. 2(b)) when there is one singularity in the low index region. Once again by simplifying the formulae given in (5), and (6) when x_2 and x_1 represent the planar interface between the higher- and lower-index layers, the following relationship is obtained for either cases:

$$\pm\mu(p_1, p_2) = \frac{\frac{1}{2}\ln\left[\frac{(p_1^2-\gamma_L^2)(p_2^2+k_H^2)}{(p_1^2+k_H^2)(p_2^2-\gamma_L^2)}\right]}{\frac{1}{2\gamma_L}\ln\left[\frac{(p_1-\gamma_L)(p_2+\gamma_L)}{(p_1+\gamma_L)(p_2-\gamma_L)}\right] - \frac{1}{k_H}\tan^{-1}\left(\frac{p_1}{k_H}\right) + \ldots \overline{\ldots \frac{1}{k_H}\tan^{-1}\left(\frac{p_2}{k_H}\right)}}$$

Since μ has no local extrema, we are left with two ways to maximize the imaginary part of the Bloch wavenumber. One way would be having $p_1 = -\gamma_L$, or $p_2 = \gamma_L$, which renders $\mu_L = \gamma_L$ for the maximum value of μ. Under such conditions, $d_H = 0$; therefore, the periodicity of the structure is killed. The other way would be letting either p_1 or p_2 approach infinity (see Figs. 2(c) and 2(d)). In such a manner, μ is maximized if the following equation is held for the finite value of $p(x)$ being named either p_0 or $-p_0$ depending on whether p_1 or p_2 approaches infinity:

$$\frac{1}{2}\ln\left(\frac{p_0^2+k_H^2}{p_0^2-\gamma_L^2}\right) = p_0\left[\frac{1}{2\gamma_L}\ln\left(\frac{p_0+\gamma_L}{p_0-\gamma_L}\right) + \frac{1}{k_H}\tan^{-1}\left(\frac{p_0}{k_H}\right) + \frac{\pi}{2k_H}\right]. \quad (9)$$

The maximum achievable μ is then equal to p_0 which will be necessarily larger than γ_L. The optimum thicknesses of higher- and lower-index layers; if there is a real p_0 satisfying equation (9), can then be obtained by using the following expressions:

$$d_H = \frac{\pi}{2k_H} + \frac{1}{k_H}\tan^{-1}\left(\frac{p_0}{k_H}\right) \quad (10\text{-a})$$

$$d_L = \frac{1}{2\gamma_L}\ln\left(\frac{p_0+\gamma_L}{p_0-\gamma_L}\right). \quad (10\text{-b})$$

The latter way of letting p_1 or p_2 to approach infinity is therefore preferable whenever equation in (9) has a real solution.

The third case is when $n_H k_0 < \beta_d$ and $k_x^2(x)$ becomes negative. We have $k_x^2(x) = -\gamma_H^2 = n_H^2 k_0^2 - \beta_d^2$ and $k_x^2(x) =$

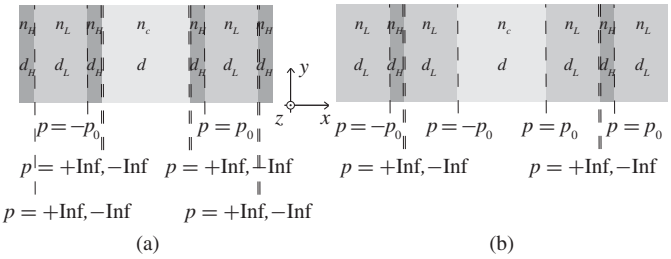

Fig. 5. (a) and (b) Two arrangements to form a planar waveguide sandwiched between optimum 1-D Bragg mirrors with the maximum Bloch confinement.

$-\gamma_L^2 = n_L^2 k_0^2 - \beta_d^2$ $(0 < \gamma_H < \gamma_L)$ in the high- and low-index layers, respectively. The pointwise wavenumber, $p(x)$, cannot be singular and we have either $\gamma_H < p_1 < p_2 < \gamma_L$ or $-\gamma_L < p_1 < p_2 < -\gamma_H$ (see Fig. 2(a)). Following the same approach, $\mu(p_1, p_2)$ can be written down as:

$$\pm\mu(p_1, p_2) = \frac{\ln\left[\frac{(p_1^2-\gamma_L^2)(p_2^2-\gamma_H^2)}{(p_1^2-\gamma_H^2)(p_2^2-\gamma_L^2)}\right]}{\frac{1}{\gamma_H}\ln\left[\frac{(p_1+\gamma_H)(p_2-\gamma_H)}{(p_1-\gamma_H)(p_2+\gamma_H)}\right] + \frac{1}{\gamma_L}\ln\left[\frac{(p_1-\gamma_L)(p_2+\gamma_L)}{(p_1+\gamma_L)(p_2-\gamma_L)}\right]}.$$

Similarly, this expression has no local extrema and the maximum μ is achieved when p_1 or p_2 takes an endpoint's value: $p_1 = \gamma_H$, $p_2 = -\gamma_H$, $p_2 = \gamma_L$, or $p_1 = -\gamma_L$. The imaginary part of the Bloch wavenumber will then be maximized when $p_2 = \gamma_L$ or $p_1 = -\gamma_L$. Under such conditions, $d_H = 0$ and the Bragg mirror region is in fact replaced with the low-index layer. In other words, it is impossible to achieve more confinement of electromagnetic waves by using the band-gap mechanism instead of total internal reflection when $n_H k_0 < \beta_d$.

B. Planar Waveguide Formed by the Optimum Bragg Mirror

Now that the optimum 1-D Bragg mirror is designed for a specific angular frequency ω_0, and propagation constant β_d, the appropriate core thickness; d, to support the highly confined Bloch wave in the optimum Bragg mirror is to be found. There are two possible arrangements to form the planar waveguide confining the light wave energy by the optimum Bragg mirror: the core region can be sandwiched by the Bragg mirror terminated with the high-index layer as is shown in Fig. 5(a), or the Bragg mirror terminated with the low-index layer as is shown in Fig. 5(b). The former shown in Fig. 5(a) is preferred because it benefits from the higher contrast between n_c and n_H, i.e., has a higher reflection at the core-cladding interface, and is more effective in confining the energy. Please notice that we are interested in waveguides with $0 \leq \beta_d < n_L k_0$ because we want to have sinusoidal distribution for electromagnetic waves in the hollow core region ($n_c = 1$). Therefore, the parameters p_0, d_H, and d_L; shown in Fig. 5, can all be obtained by using (7)–(8). The appropriate core thickness can be very easily found by applying boundary conditions at the core-cladding interface and leads to:

$$d = \begin{cases} \frac{2}{k_c}\left[m\pi + \operatorname{arccot}\left(\frac{k_c}{p_w}\right)\right] & \text{for even modes} \\ \frac{2}{k_c}\left[m\pi + \pi - \arctan\left(\frac{k_c}{p_w}\right)\right] & \text{for odd modes} \end{cases} \quad (11)$$

Here, m is an arbitrary non-negative integer denoting the mode number, $k_c^2 = n_c^2 k_0^2 - \beta_d^2$, and $p_w \to \infty$ for the structure in Fig. 5(a) or $p_w = p_0$ for the structure in Fig. 5(b). Since the even mode with $m = 0$ in the structure in Fig. 5(a) has the highest confinement, it is obvious that the appropriate core thickness of the optimum planar design is $d = \frac{\pi}{k_c}$. This relationship can be easily proved by setting $m = 0$, and $p_w \to \infty$ in (11). The fact that the core thickness in the optimum planar structure has a one-to-one relationship with the longitudinal propagation constant, β_d, at which the Bragg mirror is designed, is of utmost importance for the next section, where the core diameter of the semi-optimum Bragg fiber is to be attributed with the longitudinal propagation constant, β_d, needed for Bragg mirror design. It is worth noticing that for the planar waveguide formed by the QWS Bragg mirror [13], we have $d_H = \frac{\pi}{2k_H}$, $d_L = \frac{\pi}{2k_L}$, and $p_w \to \infty$. Interestingly, the appropriate core thickness supporting the even mode with $m = 0$ is again $d = \frac{\pi}{k_c}$.

III. Semi-Optimum Bragg Fiber with Maximum Bloch Confinement

In this section, the semi-optimum Bragg fiber with maximum confinement is proposed. The core refractive index and diameter, high and low refractive indices to be used in the cylindrical Bragg mirror, and the angular frequency of electromagnetic waves are all given and denoted by $n_c = 1$, D, n_H, n_L, and ω_0, respectively. In accordance with the parameters shown in Fig. 1, we know that $n_1 = n_H$ and $n_2 = n_L$ for the optimum Bragg fiber because the highest contrast should be achieved at the core-cladding interface. The yet unknown parameters, d_1 and d_2, in the cylindrical structure (Fig. 1(a)) are not that easy to find.

The first step would be to find the optimum values of d_1 and d_2 in the planar structure (Fig. 1(b)). The sought-after optimum values were found in the previous section but the expressions were in terms of β_d, which is not at hand. Although β_d is an unknown parameter, it can be obtained by noting that the pointwise wavenumber $p(x)$ should approach infinity at the core-cladding interface in the optimum design. Since the radial distribution of electric field within the core for the TE_{01} polarization can be written in terms of the first order Bessel function of the first kind [5], $J_1(k_c r)$, core diameter should be $D = \frac{2z_{11}}{k_c}$ [11], [14], [15], where z_{11} is the first zero of the first order Bessel function of the first kind and $k_c = \sqrt{n_c^2 k_0^2 - \beta_d^2}$. The expression $D = \frac{2z_{11}}{k_c}$ given for the cylindrical coordinate system corresponds to $d = \frac{\pi}{k_c}$ given in the previous section for the Cartesian coordinate system. It relates the core diameter D to the longitudinal propagation constant β_d needed to have the sought-after optimum thicknesses d_1 and d_2. We

TABLE I

REAL AND IMAGINARY PARTS OF THE PROPAGATION CONSTANTS FOR TE_{01}, TE_{02}, TM_{01}, HE_{11}, AND EH_{11} IN THE HERE-PROPOSED SEMI-OPTIMUM BRAGG FIBER, THE QUARTER-WAVE BRAGG FIBER, AND THE MODIFIED QUARTER-WAVE BRAGG FIBER PROPOSED IN [5], WITH: (A) TWO BILAYERS (B) THREE BILAYERS

		semi-optimum $d_H \simeq 98$ nm $d_L \simeq 182$ nm	quarter-wave $d_H \simeq 86$ nm $d_L \simeq 310$ nm	Modified quarter-wave $d_H \simeq 94$ nm $d_L \simeq 340$ nm
$\beta(1/\mu\text{m})$	TE_{01}	$4.04297694 - j0.00000045$	$4.04297133 - j0.00003441$	$4.04298007 - j0.00000266$
	TE_{02}	$4.01771663 - j0.00000281$	$4.01769317 - j0.00006314$	$4.01773263 - j0.00001363$
	TM_{01}	$4.04769340 - j0.00018100$	$4.04944205 - j0.00011839$	$4.03575929 - j0.00027179$
	HE_{11}	$4.05055695 - j0.00003637$	$4.05117977 - j0.00005436$	$4.03310908 - j0.00001739$
	EH_{11}	$4.04101194 - j0.00032570$	$4.04297085 - j0.00018904$	$4.04705316 - j0.00011039$

(a)

$\beta(1/\mu\text{m})$	TE_{01}	$4.04297173 - j0.00000005$	$4.04297106 - j0.00000267$	$4.04298924 - j0.00000022$
	TE_{02}	$4.01769914 - j0.00000032$	$4.01769680 - j0.00000493$	$4.01775909 - j0.00000115$
	TM_{01}	$4.04757836 - j0.00005145$	$4.04942284 - j0.00002237$	$4.03588134 - j0.00005645$
	HE_{11}	$4.05052426 - j0.00001018$	$4.05118162 - j0.00000822$	$4.03313061 - j0.00000290$
	EH_{11}	$4.04085638 - j0.00009292$	$4.04295068 - j0.00003553$	$4.04713541 - j0.00002217$

(b)

therefore have:

$$\beta_d = \sqrt{k_0^2 - 4z_{11}^2/D^2} \tag{12}$$

$$d_1 = \frac{\pi}{2k_1} + \frac{1}{k_1}\tan^{-1}\left(\frac{p_0}{k_1}\right) \tag{12-a}$$

$$d_2 = \frac{\pi}{2k_2} - \frac{1}{k_2}\tan^{-1}\left(\frac{p_0}{k_2}\right) \tag{12-b}$$

where $k_1 = \sqrt{n_1^2 k_0^2 - \beta_d^2}$, $k_2 = \sqrt{n_2^2 k_0^2 - \beta_d^2}$, and p_0 is the solution of the following equation:

$$\frac{1}{2}\ln\left(\frac{p_0^2 + k_1^2}{p_0^2 + k_2^2}\right) = p_0\left[\frac{1}{k_1}\tan^{-1}\left(\frac{p_0}{k_1}\right) - \frac{1}{k_2}\tan^{-1}\left(\frac{p_0}{k_2}\right) + \frac{\pi}{2k_1} + \frac{\pi}{2k_2}\right].$$

Unfortunately, the longitudinal propagation constant obtained in this manner, viz. the β_d given in (12), is not exactly equal to the actual propagation constant in the designed Bragg fiber with the specified D, d_1 and d_2. This is due to the fact that despite our design, the electric field in the cylindrical structure is not equal to the electric field in the planar structure and is thus not zero at the core-cladding interface. Therefore, the proposed design is merely a semi-optimum structure. The competence of this design in decreasing the leakage loss is in the next section compared against typical Bragg fibers. It is proved to be superior to conventional strategies for designing Bragg fibers.

Finally, please notice that we should have $\frac{2z_{11}}{k_0} < D$ to make sure that (12) is algebraically valid. This is however not a harsh constraint because $\frac{2z_{11}}{k_0}$ is usually quite small when compared against typical hollow-core Bragg fibers [5].

IV. NUMERICAL EXAMPLES

In this section, the semi-optimum hollow-core Bragg fiber proposed in the previous section is rigorously studied and its loss is compared against the loss incurred in two different types of hollow-core Bragg fibers. One type is the well-known quarter-wave Bragg fiber, whose thicknesses of high- and low-index layers in the cladding region are:

$$d_1 = \frac{\pi}{2k_1} = \frac{\pi}{2\sqrt{n_1^2 k_0^2 - k_0^2 + 4z_{11}^2/D^2}} \tag{13-a}$$

$$d_2 = \frac{\pi}{2k_2} = \frac{\pi}{2\sqrt{n_2^2 k_0^2 - k_0^2 + 4z_{11}^2/D^2}}. \tag{13-b}$$

It should be however noticed that these thicknesses are not precisely quarter-wave because; for one thing, longitudinal propagation constant and thus radial wavenumber in high- and low-index layers are not known a priori. In other words, β_d used for finding d_1 and d_2 in the abovementioned expressions is merely a good approximation based on the core diameter D. For another thing, the electromagnetic distribution is Besselian rather than sinusoidal. Hence, the concept of electrical length in the cylindrical structure is not as well defined as it is for the planar structure.

Another type of Bragg fibers employed to make a comparison against the here-proposed semi-optimum design is the one introduced in [5]. The thicknesses of high- and low-index layers in the cladding region for this type of Bragg

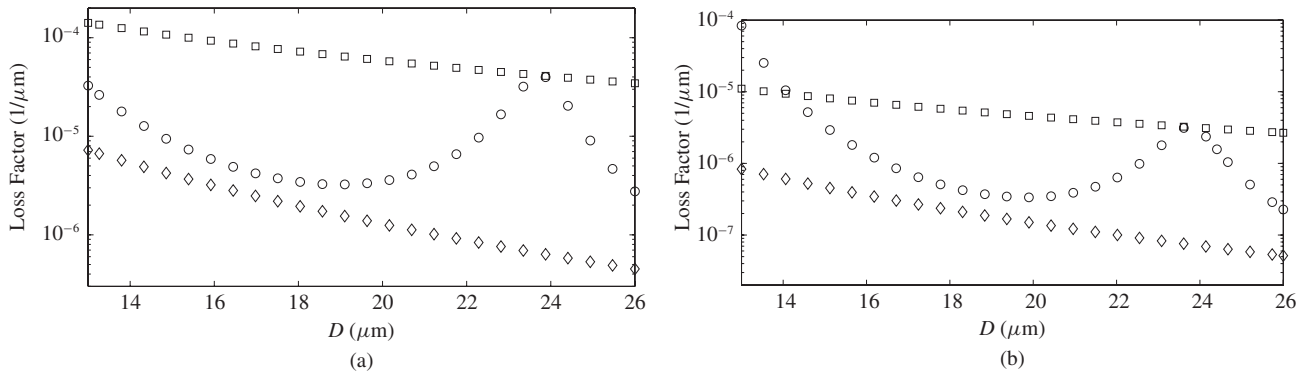

Fig. 6. TE_{01} loss factor of the semi-optimum Bragg fiber proposed here (diamond), the quarter-wave Bragg fiber (square), and the modified quarter-wave Bragg fiber (circle) versus core diameter: (a) with two bilayers and (b) with three bilayers in the cladding region.

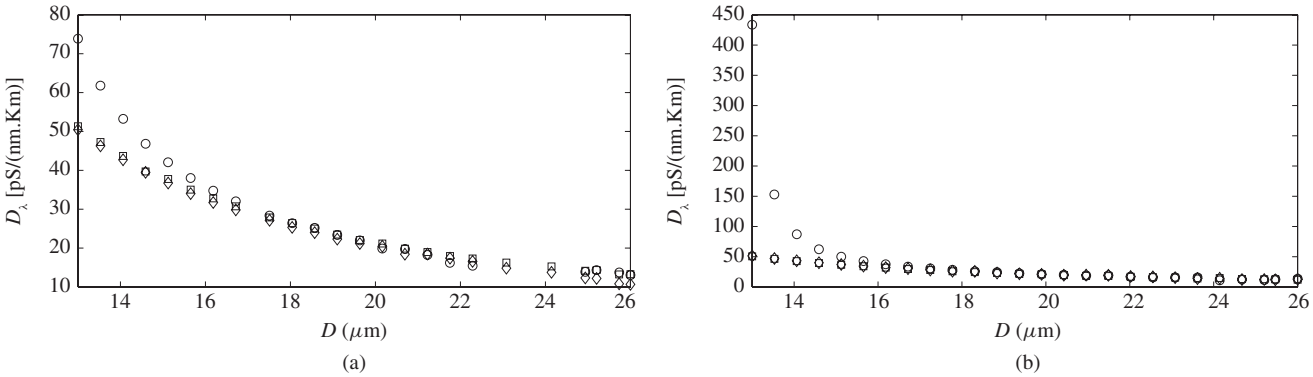

Fig. 7. TE_{01} dispersion coefficient of the semi-optimum Bragg fiber (diamond), the quarter-wave Bragg fiber (square), and the modified quarter-wave Bragg fibers (circle) versus the core diameter: (a) with two bilayers and (b) with three bilayers in the cladding region.

fibers; which is hereafter referred to as the modified quarter wave Bragg fiber, are found by solving the following equations:

$$\frac{d_1}{d_2} = \frac{\sqrt{n_2^2 - 1}}{\sqrt{n_1^2 - 1}} \tag{14-a}$$

$$D = 60(d_1 + d_2). \tag{14-b}$$

These two types of hollow-core Bragg fibers together with the here-proposed semi-optimum one are numerically analyzed for $n_H = 4.6$, $n_L = 1.6$, $D = 26.040\ \mu m$, and at the free space wavelength $\lambda_0 = 1.55\ \mu m$. These parameters have been used in [5]. The thicknesses of high- and low-index layers of the bilayer in the cladding region are $d_H = 98\ nm$ and $d_L = 182\ nm$ for the semi-optimum Bragg fiber, $d_H = 86\ nm$ and $d_L = 310\ nm$ for the quarter-wave Bragg fiber, and $d_H = 94\ nm$ and $d_L = 340\ nm$ for the modified quarter-wave Bragg fiber. On one occasion, the cladding region is considered to be made of only two bilayers and in another is made of three bilayers.

The rigorous approach is then followed; i.e., the electromagnetic fields are written in terms of Hankel and Bessel functions and the appropriate boundary conditions are duly applied to obtain the dispersion equation governing the spectral properties of longitudinal propagation constant. The sought-after longitudinal propagation constants of these fibers at the specified free space wavelength and for different polarizations are then extracted and tabulated in Table. I. In view of the fact that the cladding region is made of a finite number of bilayers, propagation constants are always complex numbers. They are extracted by following the ADR algorithm for finding complex roots of meromorphic functions presented in [16], [17].

The table clearly reveals that adding a bilayer reduces the imaginary part of the propagation constant, i.e. the loss factor. It also shows that the real part of the propagation constant does not change significantly. Furthermore, it demonstrates the superiority of the proposed semi-optimum Bragg fiber over the other two Bragg fibers. The loss factor of the dominant mode, TE_{01}, in the proposed Bragg fiber is two orders of magnitude better than the loss factor of the same mode in the quarter-wave Bragg fiber and one order of magnitude better than the same factor in the modified quarter-wave Bragg fiber introduced in [5]. It is worth mentioning that the reduction of loss factor is not bought at the expense of thicker cladding region; rather, the here-proposed semi-optimum Bragg fiber has the lowest geometrical size.

Some other TE, TM, HE, and EH modes with indices of azimuthal variation being either $m = 0$ or 1 are reported in the table. Their real parts of propagation constants happen to be very close to the real part of the TE_{01} propagation constant; and therefore, they are quite important because they can be coupling. Fortunately, the loss factor of the EH mode in the

semi-optimum design is larger than its loss factor in the other two Bragg fibers. Since the EH_{11} mode has the strongest coupling to the dominant mode, any possible unwanted coupling of energy from the dominant mode will die away at a shorter length in the semi-optimum fiber. For TE_{02}; on the other hand, the loss factor in the semi-optimum fiber is shorter than it is in the other two Bragg fibers. This is no surprise because the proposed approach minimizes the loss factor for TE polarized waves and TE_{02} is the mode with the second lowest loss factor [5].

To demonstrate how the imaginary part of the propagation constant varies with the core diameter, the loss factor of the dominant mode TE_{01} in the here-proposed semi-optimum Bragg fiber and the other two fibers are plotted versus core diameter in Fig. 6. Similar to the previous study, the constitutive parameters of all fibers are $n_H = 4.6$, $n_L = 1.6$, and the free space wavelength is $\lambda_0 = 1.55\ \mu m$. This figure clearly demonstrates that the here-proposed Bragg fiber has the lowest level of loss and that the loss factor in fibers with three bilayers are much lower than the loss factor in fibers with two bilayers. It also shows that the loss factors in the semi-optimum and the quarter-wave Bragg fibers are lower at larger core diameters. For the modified quarter-wave Bragg fiber; on the other hand, the loss factor does not monotonically decrease. The loss factor is expected to follow $\frac{1}{D^3}$ under the modified quarter-wave [5] and quarter-wave conditions [8]. In contrast, the loss factor is not proportional to $\frac{1}{D^3}$ in our case because there are only two and three bilayers. It also shows that the performance of the modified quarter-wave Bragg fiber is degraded at small core diameters.

Furthermore, the dispersion coefficients of the dominant mode in all three Bragg fibers; $D_\lambda = \frac{d}{d\lambda_0}(\frac{dRe(\beta)}{d\omega_0})$, are plotted versus the core diameter in Fig. 7. The dispersion coefficients of these fibers are not very much different from each other except for the small core diameters, when the performance of the modified quarter-wave Bragg fiber deteriorates. It should be finally noticed that the weak nonlinearity; caused by the nonlinearity of high- and low-index layers in the cladding region, and the unwanted loss; due to the imaginary part of n_H and n_L, can both be calculated by using the perturbation theory [18] in all three types of the Bragg fibers, when there is infinite number of layers and no confinement loss. The calculations show that as far as these factors are concerned, the semi-optimum Bragg fiber is slightly better than the other two; i.e. it is less prone to nonlinearity and has lower loss.

V. Conclusion

In this paper, we first found a closed form expression for the optimum thicknesses of high- and low-index layers in a planar Bragg mirror providing the maximum Bloch confinement at a given free space wavelength and propagation constant. The optimization was done by using the pointwise wavenumber based on the concept of wave admittance. The analytical optimization of the structure would be quite difficult without using this concept. It was later shown that the appropriate thickness of a hollow layer to form a planar waveguide by being sandwiched between optimum 1-D Bragg mirrors with maximum Bloch confinement can be analytically related to the propagation constant. We then modified the expression relating the propagation constant of the waveguide to the thickness of the appropriate hollow layer in a planar waveguide and found the similar expression in cylindrical structure for a hollow-core Bragg fiber. Finding an approximate expression for the propagation constant in terms of the hollow core diameter, the cladding region was optimized as if it were planar. In this fashion, a semi-optimum hollow-core Bragg fiber has been proposed to have the minimum confinement loss. The performance of this semi-optimum fiber was tested by rigorous analysis of the structure and its superiority was numerically proved.

References

[1] P. Russell, "Photonic crystal fibers," *J. Lightwave Technol.*, vol. 24, no. 12, pp. 4729–4749, Dec. 2006.

[2] P. Yeh, A. Yariv, and E. Marom, "Theory of Bragg fiber," *J. Opt. Soc. Amer. A*, vol. 68, no. 9, pp. 1196–1201, Sep. 1978.

[3] Y. Xu, G. X. Ouyang, R. K. Lee, and A. Yariv, "Asymptotic matrix theory of Bragg fibers," *J. Lightwave Technol.*, vol. 20, no. 3, pp. 428–440, Mar. 2002.

[4] J. Sakai, "Optical power confinement factor in a Bragg fiber: 1. Formulation and general properties," *J. Opt. Soc. Amer. B*, vol. 24, no. 1, pp. 9–19, Jan. 2007.

[5] S. Johnson, M. Ibanescu, M. Skorobogatiy, O. Weisberg, T. Engeness, M. Soljacic, S. Jacobs, J. Joannopoulos, and Y. Fink, "Low-loss asymptotically single-mode propagation in large-core omniguide fibers," *Opt. Exp.*, vol. 9, no. 13, pp. 748–779, Dec. 2001.

[6] G. Ouyang, Y. Xu, and A. Yariv, "Theoretical study on dispersion compensation in air-core Bragg fibers," *Opt. Exp.*, vol. 10, no. 17, pp. 899–908, Aug. 2002.

[7] A. Argyros, "Guided modes and loss in Bragg fibres," *Opt. Exp.*, vol. 10, no. 24, pp. 1411–1417, Dec. 2002.

[8] J. Sakai and H. Niiro, "Confinement loss evaluation based on a multilayer division method in Bragg fibers," *Opt. Exp.*, vol. 16, no. 3, pp. 1885–1902, Feb. 2008.

[9] C.-C. Chou and N.-H. Sun, "Analysis of leaky-mode losses for optical fibers," *J. Opt. Soc. Amer. B*, vol. 25, no. 4, pp. 545–554, Apr. 2008.

[10] D. V. Bogdanovich, "Minimization of losses and calculation of the optical properties of Bragg fiber waveguides with a hollow core," *JETP Lett.*, vol. 86, no. 4, pp. 235–239, 2007.

[11] D. V. Prokopovich, A. V. Popov, and A. V. Vinogradov, "Analytical and numerical aspects of Bragg fiber design," *Prog. Electromag. Res. B*, vol. 6, pp. 361–379, 2008.

[12] K. Rowland, S. Afshar, and T. Monro, "Bandgaps and antiresonances in integrated-ARROWs and Bragg fibers; a simple model," *Opt. Exp.*, vol. 16, no. 22, pp. 17935–17951, Oct. 2008.

[13] P. Yeh, *Optical Waves in Layered Media*. New York: Wiley, 1988.

[14] J.-L. Archambault, R. J. Black, S. Lacroix, and J. Bures, "Loss calculations for antiresonant waveguides," *J. Lightwave Technol.*, vol. 11, no. 3, pp. 416–423, Mar. 1993.

[15] J. Sakai, "Hybrid modes in a Bragg fiber: General properties and formulas under the quarter-wave stack condition," *J. Opt. Soc. Amer. B*, vol. 22, no. 11, pp. 2319–2330, Nov. 2005.

[16] L. Abd-Ellal, L. Delves, and J. Reid, "A numerical method for locating the zeros and poles of a meromorphic function," in *Numerical Methods for Nonlinear Algebraic Equations*, P. Rabinowitz, Ed. New York: Gordon and Breach, 1970, pp. 47–59.

[17] E. Anemogiannis, E. N. Glytsis, and T. K. Gaylord, "Efficient solution of eigenvalue equations of optical waveguiding structures," *J. Lightwave Technol.*, vol. 12, no. 12, pp. 2080–2084, Dec. 1994.

[18] A. Snyder and J. Love, *Optical Waveguide Theory*. New York: Chapman & Hall, 1983.

Amir M. Jazayeri (S'07–M'11) was born in Tehran, Iran, in 1985. He received the B.S. degree in electrical engineering from Sharif University of Technology (SUT), Tehran, in 2008. He was then admitted to the M.S. program in microwave and optical communications at SUT as an exceptionally talented student.

His current research interests include design, analysis, and fabrication of photonic devices for quantum information processing, bio, and communications applications, as well as novel modulation and coding techniques considering the physical nature of the communications systems.

Khashayar Mehrany (M'05) was born in Tehran, Iran, on September 16, 1977. He received the B.Sc., M.Sc., and Ph.D. (*magna cum laude*) degrees from Sharif University of Technology, Tehran, in 1999, 2001, and 2005, respectively, all in electrical engineering.

He is currently an Associate Professor in the Department of Electrical Engineering, Sharif University of Technology. His current research interests include photonics, semiconductor physics, nanoelectronics, and numerical treatment of electrical problems.